

Chapter 7

Study of a novel reaction between 2,3-dichloro 1,4-naphthoquinone and N,N'-diphenyl thiourea

7.1. Introduction

Reactions involving EDA complexes are known ; besides the references 15 -18 cited in Chapter 1 , two recent works^{143,144} of this type are involved *p*-chloranil as electron acceptor. The end products in these two reactions reveal that two vicinal Cl -atoms in *p*-chloranil are involved in the reaction . The object of the work described in this chapter is to investigate a similar possibility with 2,3-dichloronaphthoquinone (A) . This compound , because of its quinone moiety, should act as an electron acceptor¹⁴⁵ and N,N'-diphenylthiourea (B) should behave as an electron donor^{146,147} (owing to the lone pair of electrons on N). The EDA interaction between these two compounds has been studied in detail and the results are described in this chapter. It has been observed that when their solutions in chloroform, carbon tetrachloride or acetonitrile are mixed, an orange colour gradually develops. When the reaction mixture is taken in a round bottomed flask covered in thick black cloth and heated, HCl is liberated (which was tested by conventional methods viz., holding moist litmus paper and glass rod moistened with ammonia in the issuing gas). The reaction occurs both thermally and photochemically, the latter being more rapid: when the reaction mixture is kept in bright sunlight orange colour develops in about ten minutes. By column chromatography on silica gel, two final products, one orange in colour and the other violet, have been isolated in pure form and characterised. A detailed kinetic study of both the dark(thermal) and photochemical paths have been carried out. Results are described in the following sections.

7.2. Isolation of the final products:

A mixture of (A) and (B) in a mole ratio \approx 1:1 in acetonitrile was refluxed for 4 hrs. in the dark. The brown coloured solution , after filtration , was extracted with aqueous 2% NaOH solution to remove the unreacted naphthoquinone and then subjected to chromatographic separation on silica gel ; eluents used were successively petroleum ether(PE), and 10% , 20% , and 30% mixtures of benzene (Bz) and PE. The orange coloured compound (X) was collected in the 20% Bz in PE fraction and the violet compound (Y) in the 30% Bz in PE fraction.

7.3. Characterisation of the final products X and Y.

At first the stoichiometric ratio B : A required for the formation of the orange coloured product X was determined by Job's method of continuous variation . Mixtures containing the same total concentration of B and A but different molar ratios (in acetonitrile medium) were kept in the dark for 12 hrs. and their absorbances were measured at 473 nm (the λ_{\max} of the isolated X) using a Shimadzu UV-VIS 2101PC spectrophotometer fitted with a TB-85 thermo bath . Experimental data (Table 7.1) indicate that a mole ratio A : B = 1:1 is required for the formation of X. The violet compound Y is probably formed by a photochemical decomposition of X during chromatography on silica gel .

Table 7.1. Data for Job type experiment recorded after keeping the mixture in the dark for 12 hrs.

$10^3 [A]_0 / \text{mol.dm}^{-3}$	$10^3 [B]_0 / \text{mol.dm}^{-3}$	$[B]_0 / ([A]_0 + [B]_0)$	Absorbance at $\lambda = 473 \text{ nm}$
0.9301	8.3712	0.90	0.111
1.8603	7.4411	0.80	0.125
2.7904	6.5109	0.70	0.139
3.7205	5.5808	0.60	0.153
4.6507	4.6507	0.50	0.218
5.5808	3.7205	0.40	0.152
6.5109	2.7904	0.30	0.150
7.4411	1.8603	0.20	0.145

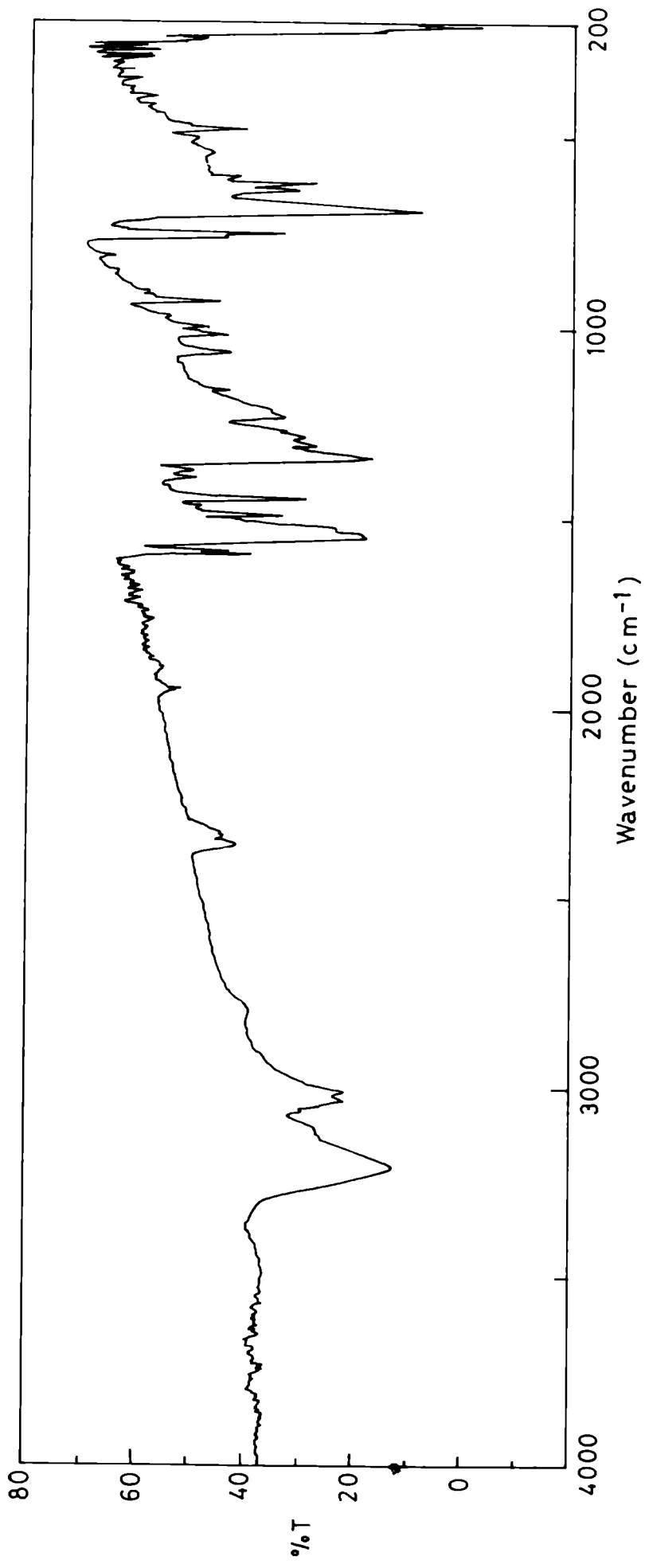


Fig.7.1. IR spectrum of N,N'- diphenyl thiourea

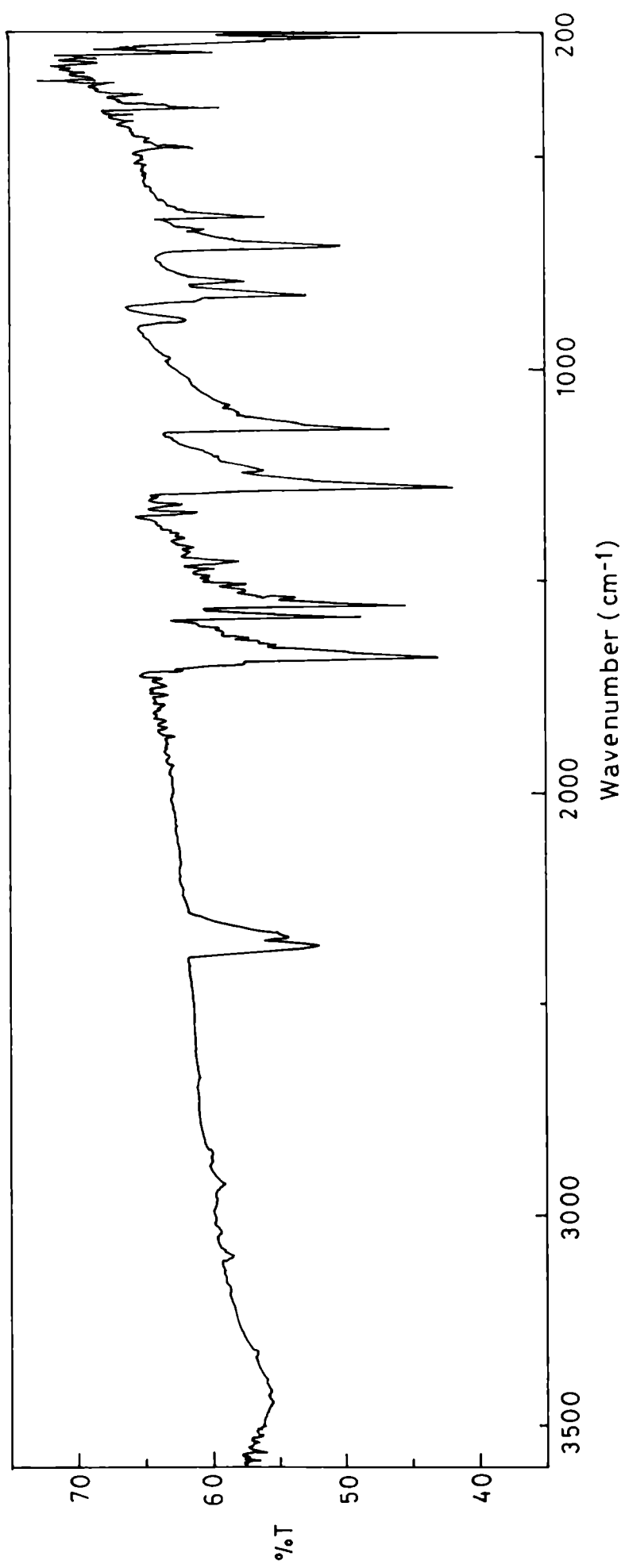


Fig.7.2. IR spectrum of 2,3-dichloro 1,4-naphthoquinone

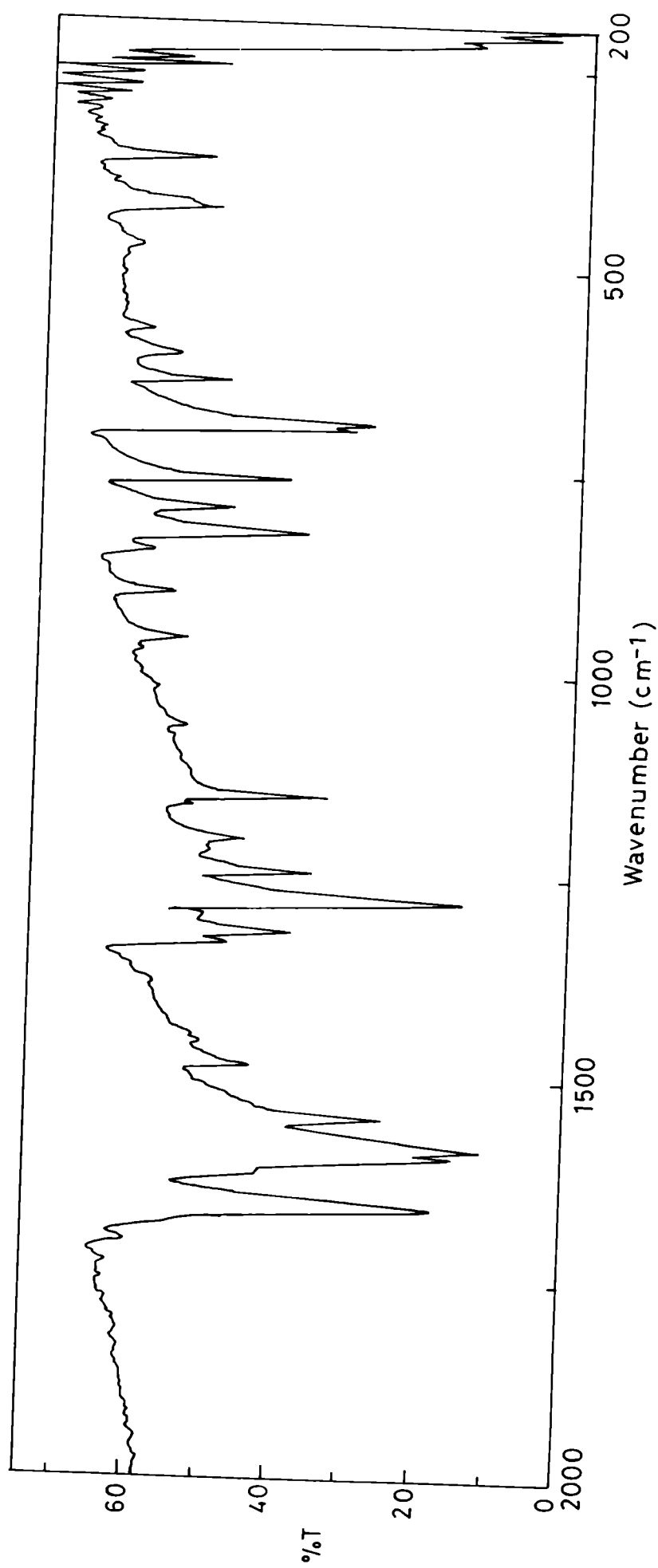


Fig. 7.3. IR spectrum of the orange coloured product (X), 2,3-(N,N'-diphenylthioureylene)-naphtho-1,4-quinone.

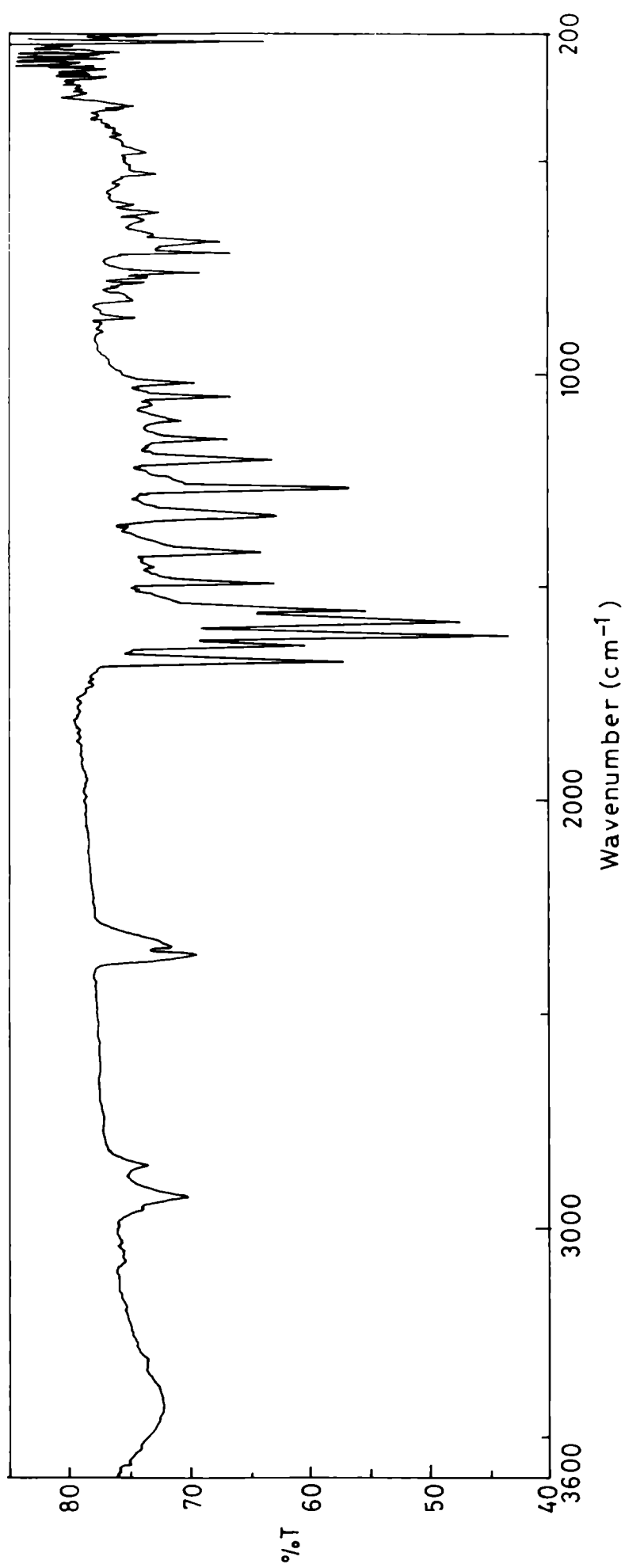


Fig.7.4. IR spectrum of the violet compound (Y), 2,3-(N-phenyl-[2', 3'] benzo epimino) naphtho-1,4-quinone.

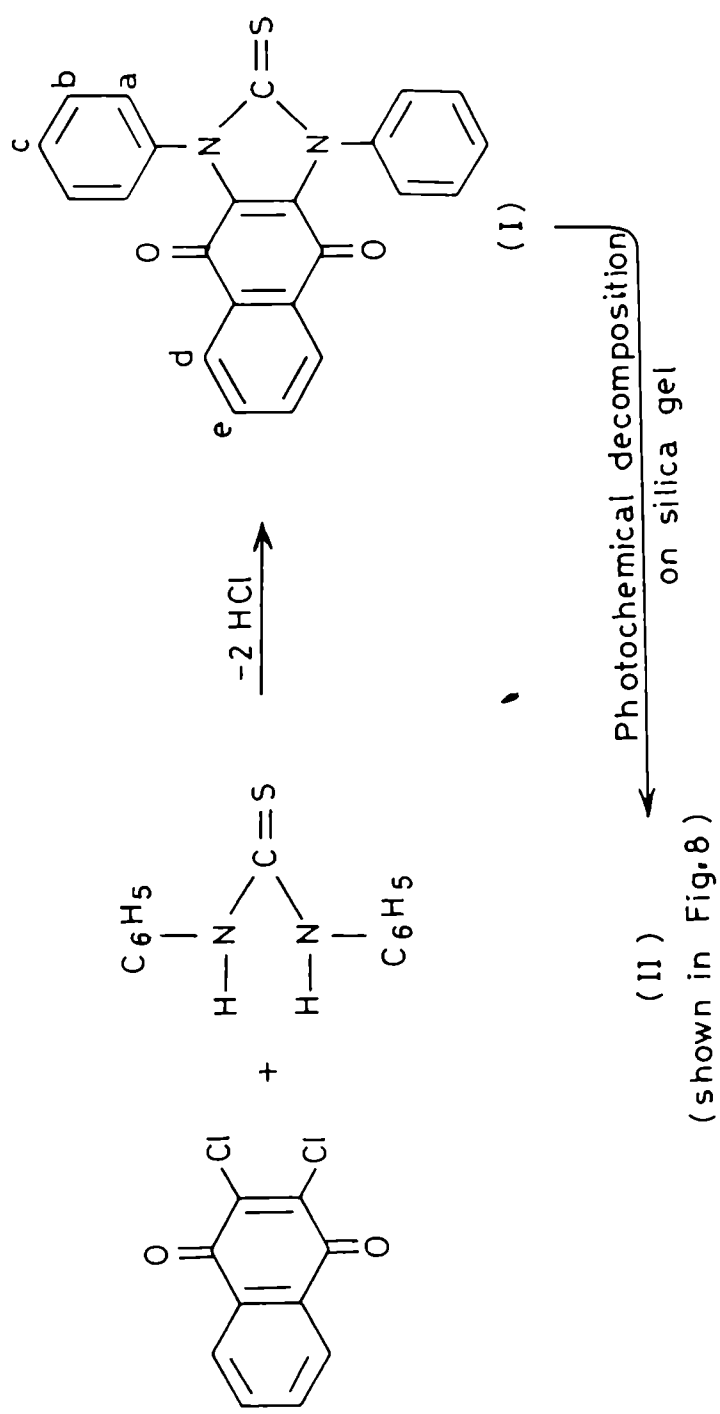


Fig.7.5. A plausible reaction path and structures of the final products.

The IR spectra (KBr pellet) of the reactants (A) and (B) and of the two products (X) and (Y) were recorded on a JASCO FT/IR -420 instrument and are shown in Figs. 7.1-7.4 . The 3207 and 3035 cm^{-1} bands observed with (B) are due to N-H stretch (as compared with the 3400 and 3300 cm^{-1} bands for this mode of vibration observed with 2-thiourea¹⁴⁸) . These two bands are totally absent in the spectra of X and Y. The C = O stretching band (1681 cm^{-1}) observed with the reactant (A) appears at 1661 cm^{-1} and 1676 cm^{-1} respectively in X and Y. Since the C=O stretch in case of 1,4 naphthoquinones is expected¹⁴⁹ in the range 1690 - 1660 cm^{-1} , we may conclude that the naphthoquinone moiety of (A) is retained in the products (X) and (Y).

By conventional method (ie, fusion with metallic sodium, extraction with water followed by testing with sodium nitroprusside solution) sulphur was found to be present in the orange compound (X) and absent in the violet compound (Y).

The disappearance of the 3207 and 3035 cm^{-1} N-H stretching bands in the IR spectra of X and Y, the observation of elimination of HCl during reaction and the results of elemental analysis lead to the proposition of structures I and II for X and Y respectively according to the reaction scheme given in Fig. 7.5.

The proposed structures are consistent with elemental analysis results: X (i.e., $\text{C}_{23}\text{H}_{14}\text{N}_2\text{O}_2\text{S}$) expects C 72.25%, H 3.66% , N 7.33% ; found C 72.15% , H 3.65% , N 7.34% . Y (i.e., $\text{C}_{22}\text{H}_{13}\text{NO}_2$) expects C 81.73% , H 4.02% , N 4.33% ; found C 81.71% , H 4.01% , N 4.37% .

The electron impact mass spectra of X and Y are shown in Figs. 7.6 and 7.7 respectively . In case of X, the P, P+1 and P+2 peaks are observed at two different fragment peaks, viz., at $m/e = 323$ and at 135. This indicates the presence of S atom . In the molecular ion peak (382) the P+1 and P+2 peaks are too weak to be detected . The even molar mass indicates the presence of an even number of N atoms per molecule of X. The base peak at 323 is probably due to expulsion of HCNS from the molecule I (Fig. 7.5) ; the relative abundance of the P+2 peak (325) is too high to be accounted for by one S atom . The peaks at m/e 135, 136, and 137 are due to the resonance stabilised $[\text{C}_6\text{H}_5 \text{ CNS}]^+$ fragment. Expulsion of $[\text{C}_6\text{H}_5 \text{ CNS}]$ from the molecular ion followed by removal of one CO molecule leads to the fragment with m/e 219.

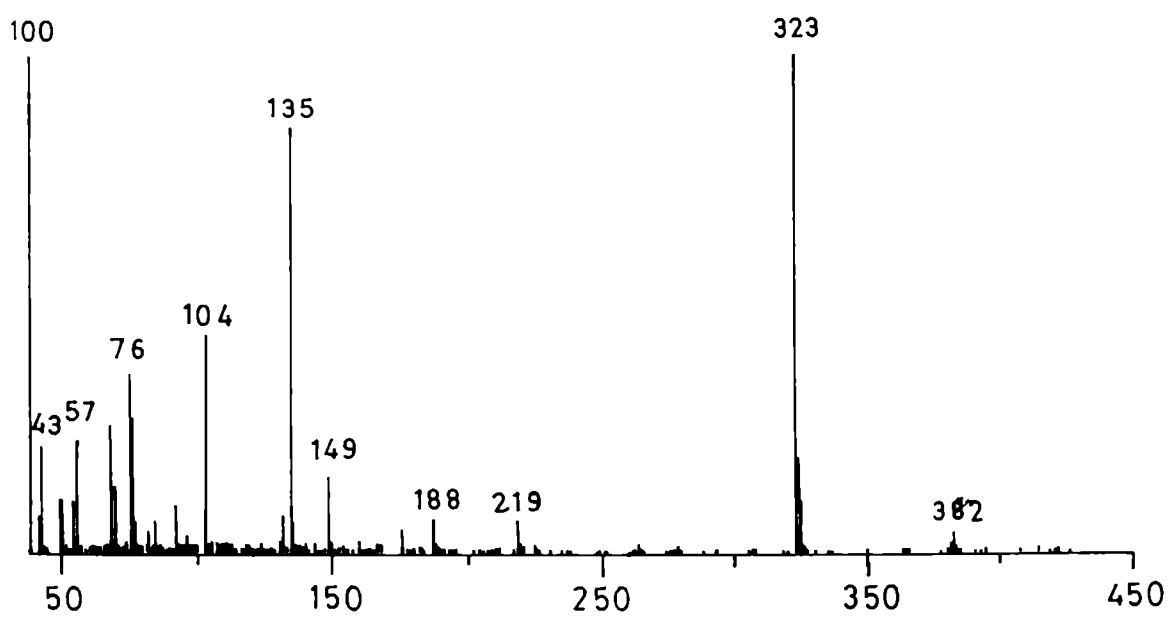


Fig.7.6. Electron impact mass spectrum of the compound (X).

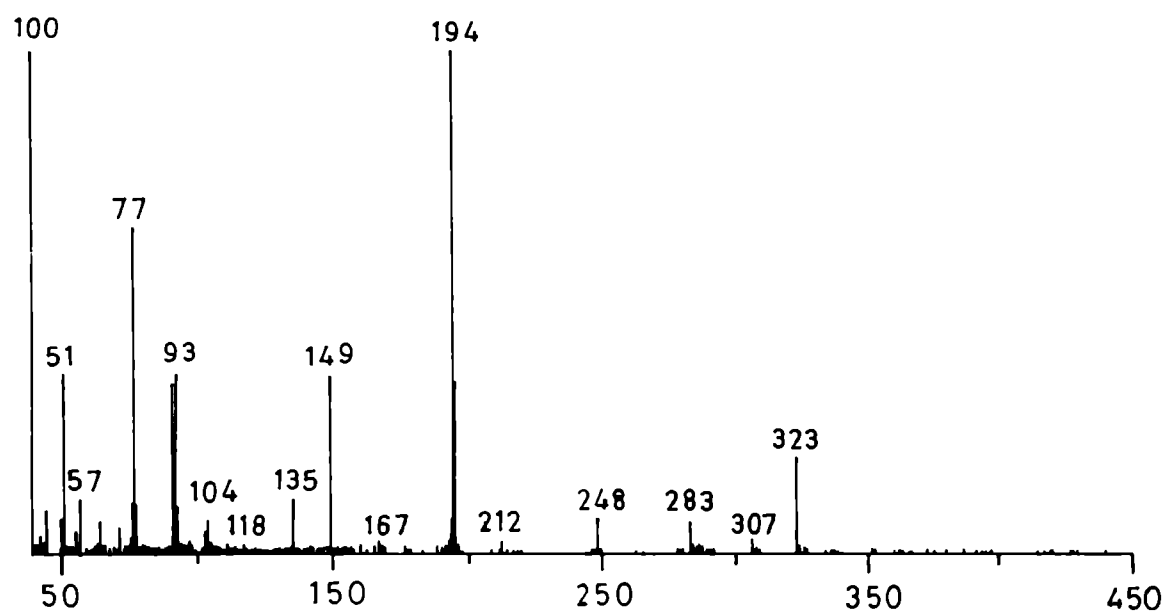


Fig.7.7. Electron impact mass spectrum of the compound (Y).

In case of Y there are P(194), P-1 and P+1 peaks but no P+2 . This indicates the absence of S in Y. The expulsion of HCNS from a molecule of X (structure I, Fig. 7.5) may occur along the plausible route shown in Fig. 7.8. This process which occurs in the mass spectrometer by electron impact may also occur photochemically . Thus a plausible structure for Y is II. The fragment with m/e 248 is a result of expulsion of C₆H₅ from II followed by incorporation of 2 protons (323-77+2= 248). The base peak 194 may be attributed to the expulsion of C₆H₅ followed by two C₂H₂ molecules (323-77-52= 194). These assignments are based on the fact that expulsion of CO and acetylene from 1,4-naphthoquinones is a common phenomenon in mass spectrometry¹⁵⁰.

The ¹H (300 MHz) and ¹³C (75.5 MHz) spectra of the compounds X and Y were recorded with a Bruker AM-300L superconducting magnet NMR spectrometer using a 5 mm ¹H -¹³C dual probe and operating with Bruker DISR 861 software (solvent CDCl₃ , internal standard TMS). The proton NMR spectrum of X (Fig. 7.9) shows signals in the aromatic region and DEPT reveals five branches at δ 7.7 (m, J=6.0 and 3.0Hz), δ 7.4 (dd, J=11.4 Hz) , δ 7.2 (J=9.0Hz) and δ 7.0 (m, J= 2.1 and 10.8 Hz). These may be attributed to the protons at the positions a to e respectively as shown in structure I (Fig. 7.5). All the protons of Y (Fig.7.10) also resonate in the aromatic region and in this case DEPT reveals nine distinct branches at δ 8.08 (m, J = 6.0, 3.6, 2.1 and 1.5 Hz), δ 7.95 (m, J=5.7, 3.3, 2.4 and 2.1Hz), δ 7.75 (m, J=8.4, 6.9, 3.9, 3.6, 3.0, 2.4 and 2.1 Hz), δ 7.53 (m, J=6.3, 5.1, 3.3 and 2.7 Hz), δ 7.37 (m, J= 7.2, 3.9, 3.3, 2.7, 2.4 and 2.1 Hz), δ 7.30 (d), δ 7.10 (dd, J=11.1Hz), δ 6.98 (t, J=3.0, 1.8 Hz) and δ 6.94 (dd, J=1.7 Hz). These may be attributed respectively to the protons at positions p-x indicated in structure II (Fig. 7.8). The ¹³C NMR spectra of X and Y are shown in Figs. 7.11 and 7.12 . Y exhibits sixteen signals corresponding to sixteen non-equivalent carbon atoms in structure II. The number of signals in X is much less owing to symmetry . The resonance at δ_c = 150 ppm which is observed with both the compounds, is due to the carbonyl carbon and those in the range δ_c =120 to 128, observed with both the compounds, are attributable to the C -atoms in the heteroaromatic five-membered ring¹⁵¹.

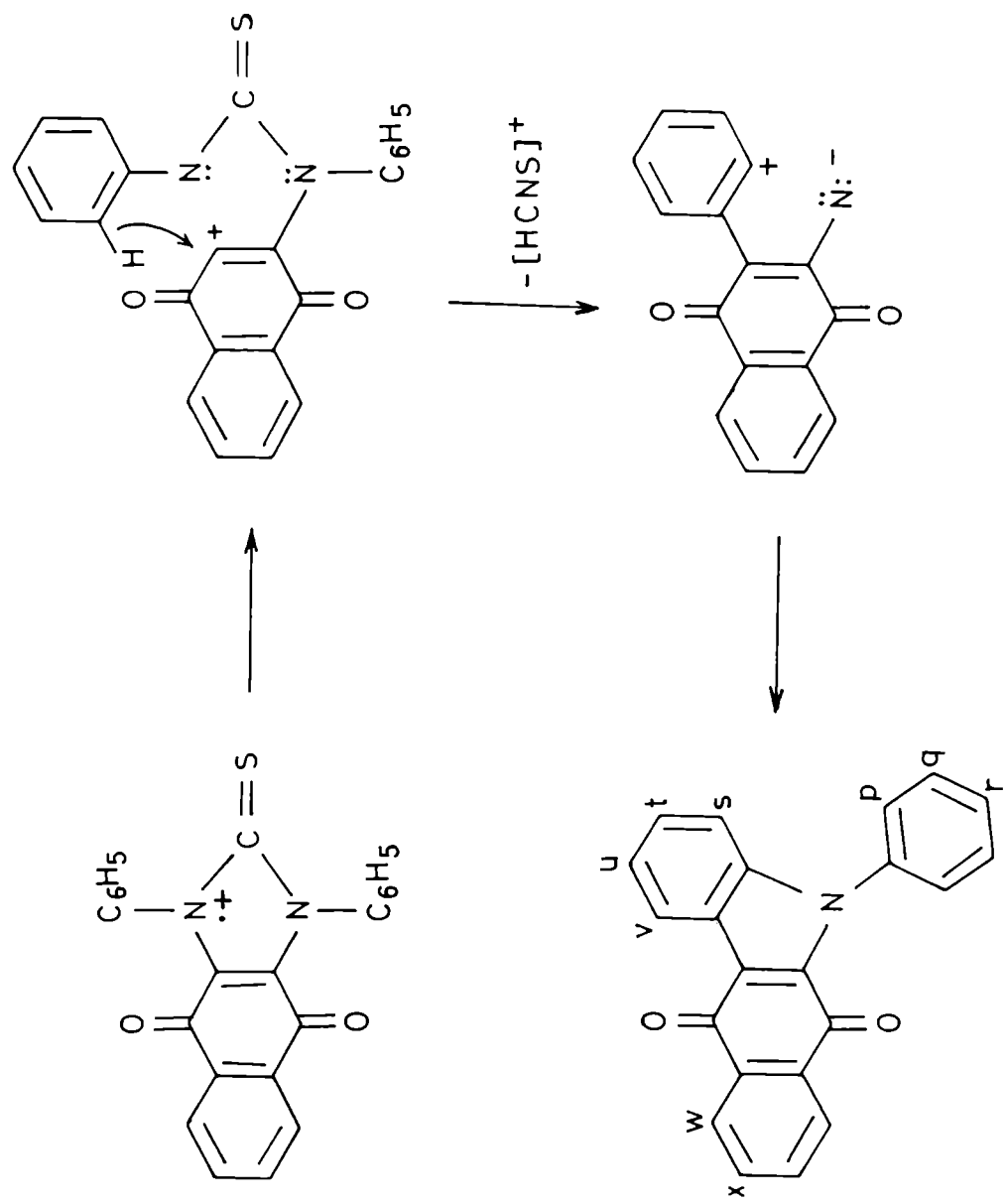


Fig.7.8. A plausible route for the formation of compound (Y) from (X).

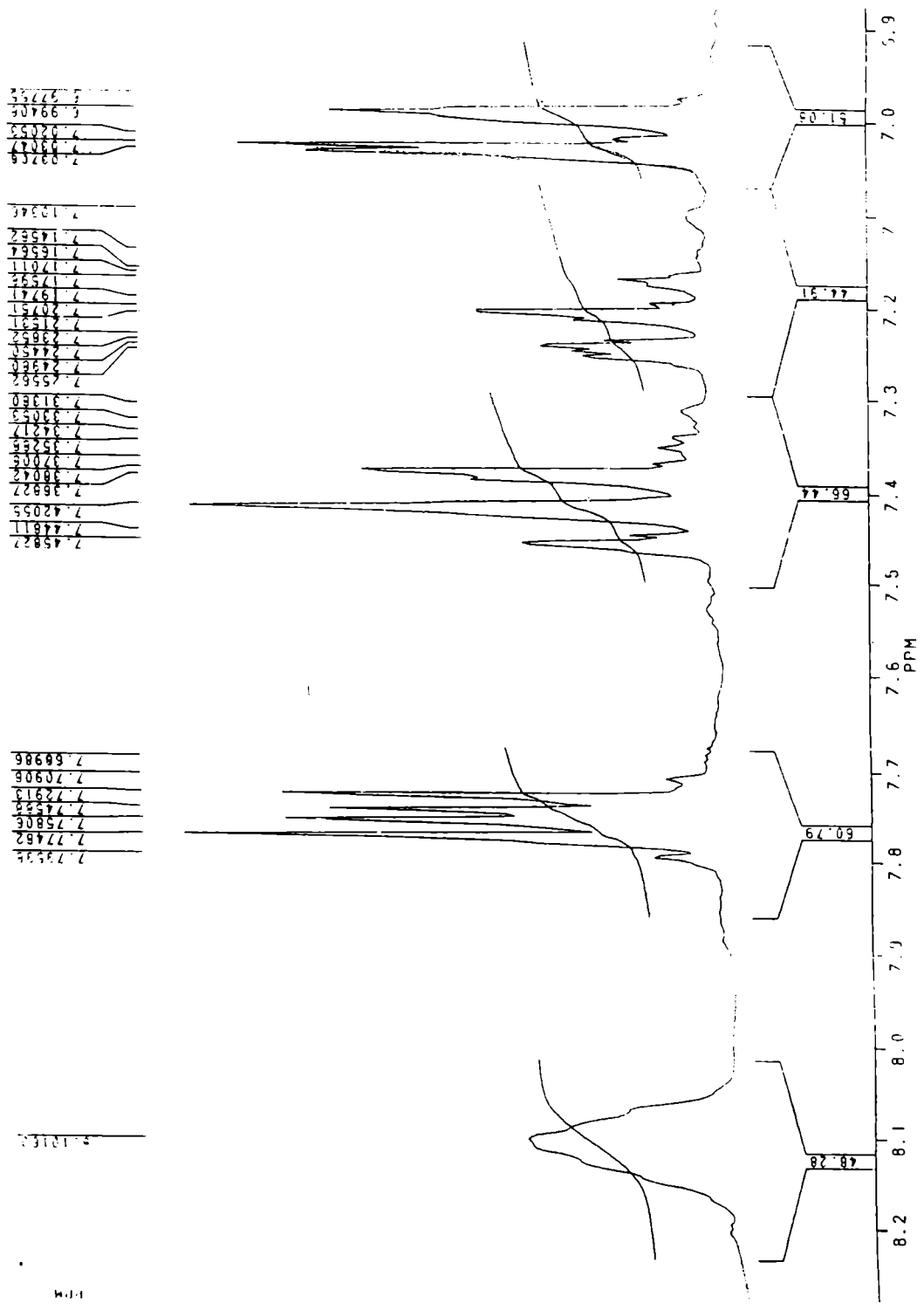


Fig.7.9. ¹H NMR spectrum of the compound (X).

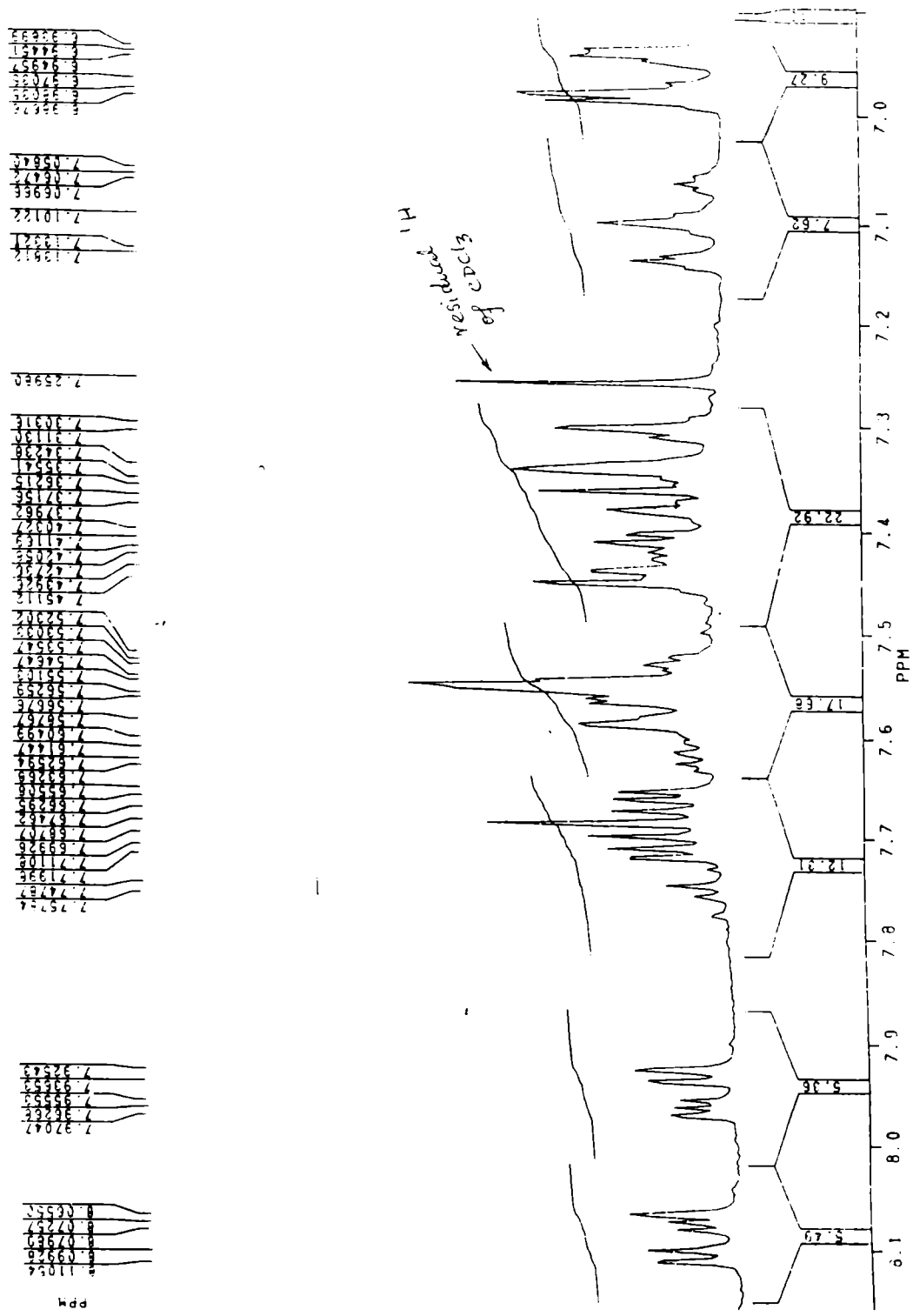


Fig.7.10. ¹H NMR spectrum of the compound (Y).

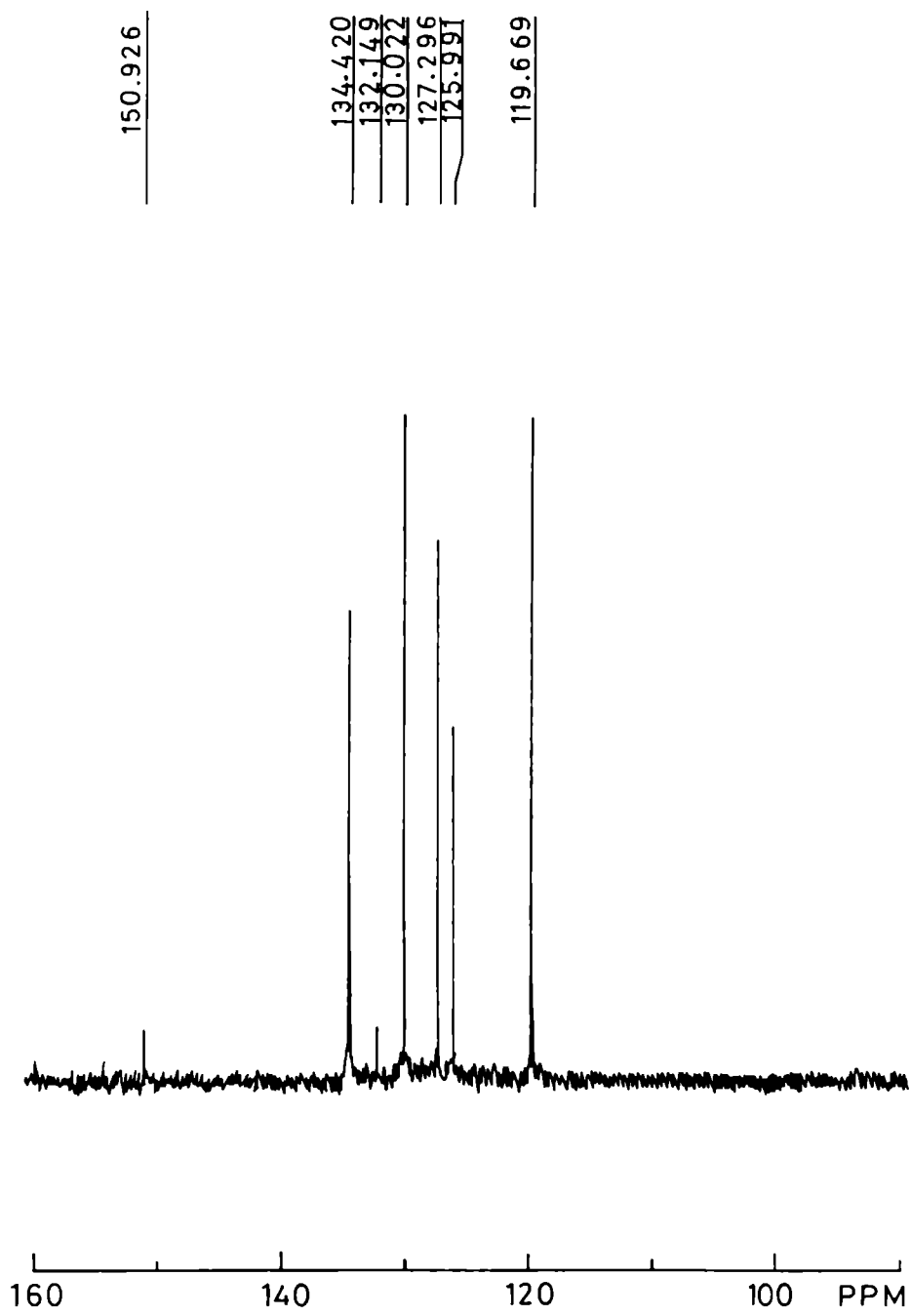


Fig.7.11. ^{13}C NMR spectrum of the compound (X).

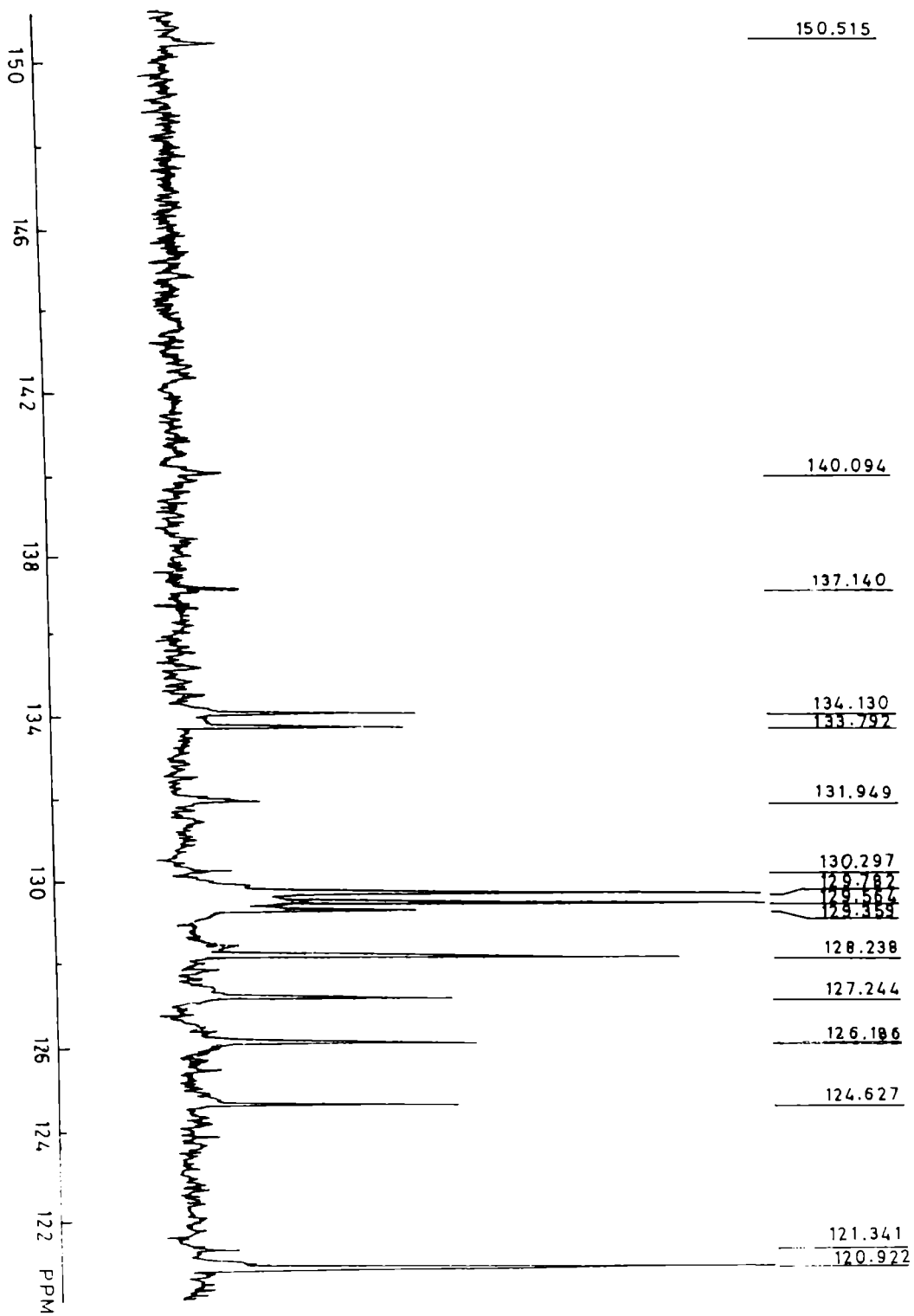


Fig. 7.12. ^{13}C NMR spectrum of the compound (Y).

As regards electronic absorption spectra the wavelengths at the absorption maxima and the corresponding molar absorptivities(ϵ) of the compounds in a number of solvents are given in Table 7.2.

Table 7.2. Electronic spectral data for X and Y

solvent	X	Y
	λ_{\max} /nm , (ϵ)	λ_{\max} /nm , (ϵ)
Methanol	475 (1453)	510 (1797)
Acetonitrile	473 (1993)	514 (819)
Chloroform	491 (1713)	527 (5449)
Carbon tetrachloride	487 (1668)	523 (1754)
n-heptane	482 (1392)	523 (1414)

7.4. Kinetic study of the reaction

Kinetics of the reaction has been followed spectrophotometrically in acetonitrile medium. When mixtures of (A) and (B) at concns. $\sim 10^{-2}$ mol. dm^{-3} are kept in the dark (within the closed chamber of the spectrophotometer) and their spectra are recorded at regular time intervals, a broad absorption band is found to develop slowly (Fig. 7.13). When the same mixture is exposed to diffused sunlight, the orange colour develops relatively rapidly. This indicates that the reaction occurs both thermally and photochemically, the latter path being more rapid. Data in Table 7.3 and Fig. 7.14 reveal this more clearly. The kinetic study has, therefore, been carried out separately for the thermal and photochemical paths and the results are discussed in the following sections.

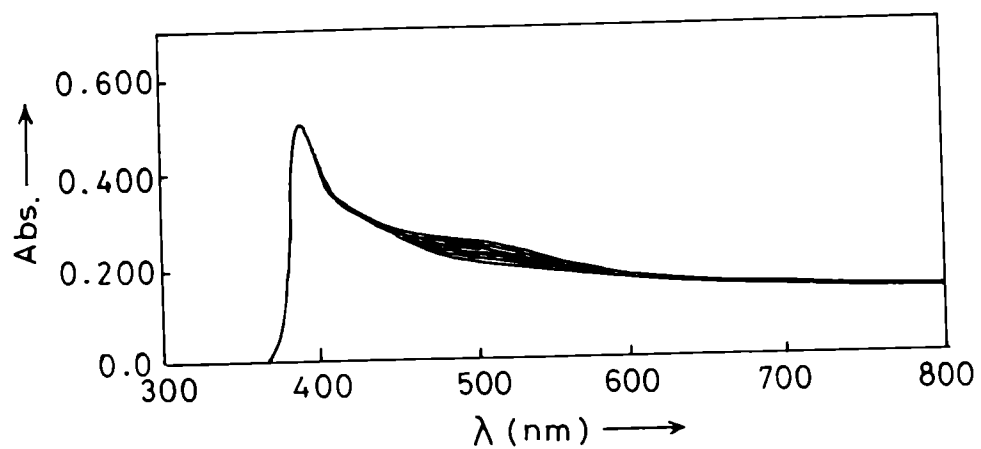


Fig.7.13. Variation of the absorption spectrum of a mixture of A and B in CH₃CN with time. $[A]_0 = 4.727 \times 10^{-3} \text{ mol.dm}^{-3}$ and $[B]_0 = 5.806 \times 10^{-2} \text{ mol.dm}^{-3}$ in mixture. Intensity of the broad band increases with time.

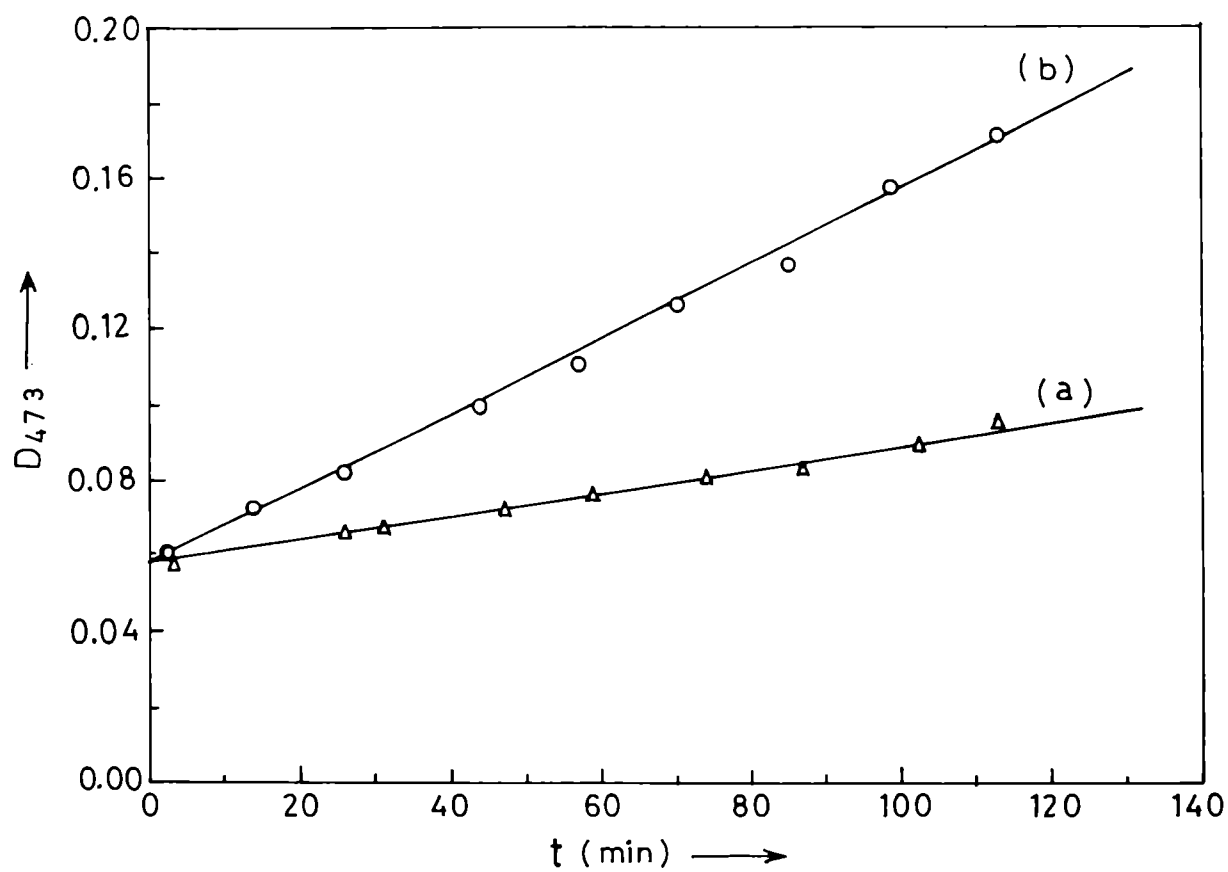


Fig.7.14. Variation of absorbance of the reaction mixture at 473 nm with time in the thermal(a) and photochemical (b) paths. Initial concentrations are as indicated in Table 7.3

7.5. Kinetic study of the thermal (dark) path .

Variation of absorbance at 473 nm of A+B mixtures in acetonitrile with time was recorded at four different temperatures. Data at one temperature (297K) are given in Table 7.3 . Those at three other temperatures are given in Table 7.4 .

Table 7.3. Variation of absorbance of a mixture of (A) and (B) in acetonitrile in the thermal and photochemical paths at 297K . $[A]_0 = 1.049 \times 10^{-2} \text{ mol.dm}^{-3}$ and $[B]_0 = 3.1329 \times 10^{-2} \text{ mol.dm}^{-3}$

Thermal		Photochemical	
time /min	absorbance* at 473** nm	time /min	absorbance at 473 nm
3	0.058	2	0.060
15	0.062	14	0.072
26	0.065	26	0.082
31	0.067	44	0.100
47	0.072	57	0.111
59	0.075	70	0.126
74	0.080	85	0.137
87	0.083	99	0.158
103	0.089	113	0.172

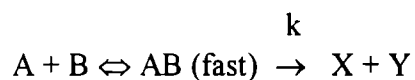
* Measured against the solution of A as reference ; B is colourless and does not absorb at 473 nm.

** the λ_{max} of isolated X.

Table 7.4. Variation of absorbance of A+B mixtures in acetonitrile at 473 nm at three different temperatures.

$[A]_0 / \text{mol} \cdot \text{dm}^{-3}$	$[B]_0 / \text{mol} \cdot \text{dm}^{-3}$	Temp. /K	Time /min	Absorbance
3.9158×10^{-3}	4.759×10^{-2}	303	8	0.032
			18	0.033
			28	0.034
			38	0.034
			48	0.035
			58	0.036
			70	0.037
			78	0.038
			88	0.039
			98	0.040
6.1056×10^{-3}	5.428×10^{-2}	310	13	0.059
			21	0.060
			27	0.062
			35	0.063
			43	0.064
			48	0.066
			52	0.067
			58	0.068
			63	0.070
5.0344×10^{-3}	4.079×10^{-2}	316	10	0.036
			14	0.037
			18	0.038
			23	0.039
			28	0.040
			43	0.044
			49	0.046
			55	0.047
			58	0.048
			63	0.050
68	0.051			

Owing to the low solubility of 2,3-dichloro 1,4-naphthoquinone (A) , the usual method of isolation for determination of the pseudo-order of the reaction with respect to N, N'-diphenyl thiourea could not be determined . Moreover , it was found that the rate depends on the product $[A]_0 [B]_0$ of the initial concentrations of A and B. Out of a number of plausible reaction schemes, the experimental data fit well to



Rate of formation of products is given by

$$d[X] /dt = d[Y] /dt = - d[AB] /dt = k[AB] \quad \dots (7.1)$$

where square brackets indicate concentrations . This on integration gives

$$[AB] = [AB]_0 e^{-kt} \quad \dots (7.2a)$$

$$\text{and } [X] = [Y] = (1 - e^{-kt}) [AB]_0 \quad \dots (7.2b)$$

where the subscript 0 stands for $t = 0$.

With a cell of path length 1 cm , the absorbance at 473 nm is

$$\begin{aligned} D^{473} &= \epsilon_{AB} [AB] + \epsilon_X [X] + \epsilon_Y [Y] \\ &= M e^{-kt} + N \quad \dots (7.3) \end{aligned}$$

where

$$M = (\epsilon_{AB} - \epsilon_X - \epsilon_Y) [AB]_0 \quad \dots (7.4)$$

and

$$N = (\epsilon_X + \epsilon_Y) [AB]_0 \quad (7.5)$$

and the ϵ terms are the molar absorptivities of the substances indicated at the suffixes.

As the data in the Table 7.3 for the thermal reaction indicates, the decay constant k is small and so e^{-kt} can be approximated to $(1 - kt)$. Thus,

$$D^{473} \approx (M + N) - Mkt \quad \dots (7.6)$$

Hence plot of D^{473} vs t should be linear with

$$\text{intercept, } M + N \approx \epsilon_{AB} K [A]_0 [B]_0 \quad \dots (7.7)$$

and

$$\text{slope} = -Mk \approx K k [A]_0 [B]_0 (\epsilon_X + \epsilon_Y - \epsilon_{AB}) \quad \dots (7.8)$$

which yield ,

$$\text{slope / intercept} = [k (\epsilon_X + \epsilon_Y - \epsilon_{AB})] / \epsilon_{AB} = k \epsilon_r \quad \dots (7.9a)$$

$$\text{intercept} / [A]_0[B]_0 = K \epsilon_{AB} \quad \dots (7.9b)$$

where $\epsilon_r = (\epsilon_X + \epsilon_Y - \epsilon_{AB}) / \epsilon_{AB}$ is a constant which may be taken to be independent of temperature .

Fig. 7.14(a) shows the validity of eqn. (7.6). Similar plots were obtained with data at all the other temperatures . Positive slope indicates that $\epsilon_X + \epsilon_Y > \epsilon_{AB}$ at 473 nm. Values of $k \epsilon_r$ and $K\epsilon_{AB}$ obtained from such plots are summarised in Table 7.5 . It was found that $\ln (K\epsilon_{AB})$ correlated well with $1/T$ according to the linear equation,

$$\ln (K\epsilon_{AB}) = 329.3 / T + 4.04 \quad \dots (7.10)$$

with a correlation coefficient of 0.91. This gives -0.70 ± 0.19 Kcal. mol⁻¹ as the enthalpy of formation of AB ; This value is consistent with heats of formation of typical EDA complexes (see p. 106 of ref. 17) . The variation of $k\epsilon_r$ with temperature, however , is not accurate enough for determination of enthalpy of activation .

Table 7.5. Rate constant of the decay process and formation constant of the AB adduct.

Temp / K	$k \epsilon_r \times 10^3$	$K\epsilon_{AB}$	ΔH_f
297	5.24	174	- 0.70± 0.19 Kcal.mol ⁻¹
303	2.89	167	
310	3.77	168	
316	7.84	161	

7.6. Study of the photochemical path

While DPTU has no absorption in the visible range, the acceptor in CH₃CN medium has a weak n-π* absorption band peaked at 360 nm, the molar absorptivities at 360, 365 and 370 nm being respectively 188, 148 and 112. The quantum yields of the reaction have been determined at these wavelengths with available light sources.

a) Using ordinary monochromatic light source

The intensity of a cylindrical light beam from a monochromatic UV source (λ = 360 nm) was measured by potassium ferrioxalate actinometry (using the standard method stated in reference 152). The value of the intensity of that light source is 1.9950 × 10⁻⁵ einstein lit⁻¹ min⁻¹.

A mixture containing 1.284 × 10⁻² mol.dm⁻³ of [A] and 4.004 × 10⁻² mol.dm⁻³ of [B] in acetonitrile was exposed to the same light beam incident normally to the reaction mixture, the optical path length through the reaction mixture being 1 cm. The concentration of the product (X) formed after irradiation was determined by measuring the absorbance of the irradiated solution at 473 nm, the wavelength of maximum absorption of X (Y has no appreciable absorption at this wavelength). Experimental data and results are given in Table 7.6.

The plot of absorbance against exposure time is fairly linear (Fig. 7.15) and its slope, when divided by the molar absorptivity (1993) of X at 473 nm, gives the rate of formation of X. Then the quantum yield of the reaction comes out to be

$$\begin{aligned} \phi &= (d[X] / dt) / I_{\text{abs}} = [(\text{slope of Fig. 13a}) / 1993] / [I_0 (1 - 10^{-\epsilon [A]})] \quad (l = 1 \text{ cm.}) \\ &= 0.26 \quad (7.11) \end{aligned}$$

b) Using 365 nm and 370 nm laser beams

Quantum yields of the same reaction were determined using laser sources at 365 and 370 nm. These were obtained by non-linear optical frequency mixing technique ($1/\lambda_1 + 1/\lambda_2 = 1/\lambda_3$). 1064 nm. (λ₁) radiation from an electro-optically θ - switched Nd:YAG laser (model DCR-11 of M/S Spectra Physics, USA, pulse width 10 ns, repetition ratio 10 Hz) was mixed with 555.6 nm and 567.3 nm (λ₂) respectively from a 532 nm pumped dye laser

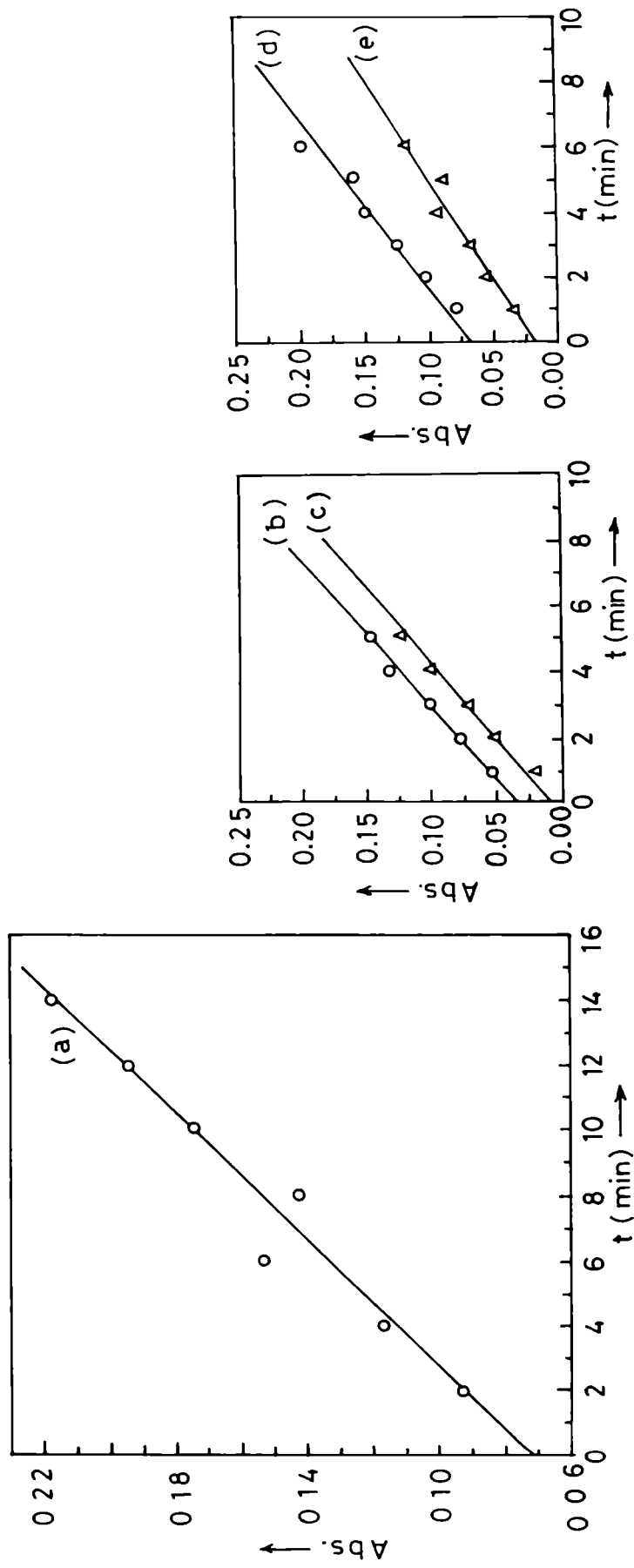


Fig.7.15. Plots for determination of quantum yield. (a): ordinary UV source($\lambda = 360$ nm), (b) and (c): laser source ($\lambda=365$ nm) with two different initial concentrations of reactants. (d) and (e) : laser source ($\lambda=370$ nm) at two different initial concentrations of reactants. Concentrations are as indicated in Table 7.6

(model PDL - 2 of M/S Spectra Physics , USA). The dye solution used was Rhodamine 570 tunable from 553- 577 nm . The mixing was done on a beta barium borate (BBO) crystal . The unconverted 1064 nm and the dye radiations were blocked by UV glass fitters and the desired laser beam (365 and 370 nm separately) was allowed to fall normally on a quartz cell (path length = 0.5 cm) containing the reaction mixture (A+B in CH₃CN) . Diameter of the beam used was 3 mm. in each case. Immediately after exposure to the beam, the absorbances of the irradiated solutions at 473 nm were measured . In each case 1.1 ml of reaction mixture was taken for irradiation . Experimental data are given in Table 7.6. Upto 6 mins. of irradiation , the plot of absorbance at 473 nm against exposure time is linear as shown in Fig. 7.15 . The slope of each line when divided by the molar absorptivity (1993) of X at 473 nm gives an apparent rate of formation of X . This has to be multiplied by the factor (1.1/0.5πr²) in order to get the actual d[X]/ dt . This is because the portion of the solution actually irradiated diffuses into the entire bulk before recording the absorbance .

Now since the incident beam consists of 10 ns pulsed laser , the quantum yield is obtained from

$$\phi = [d[X] /dt] /60 \times 10^{-8} I_{\text{abs}} \quad (7.12)$$

where

$$I_{\text{abs}} = [\text{peak power in einstein} \cdot \text{sec}^{-1}] / (1-10^{-\epsilon[A]l}) \quad (7.13)$$

Here l = 0.5 cm and ε is the molar absorptivity of A at the wavelength of the incident radiation . Values of φ thus obtained are shown in Table 7.6 .

Table 7.6. Data for determination of quantum yield

Source (intensity, I_0)	$10^2 \times [A]$ (mol.dm ⁻³)	$10^2 \times [B]$ (mol.dm ⁻³)	Exposure time (min)	Absorbance at $\lambda = 473$ nm	Quantum yield
360 nm , ordinary beam ($I_0 = 1.9950 \times 10^{-5}$ einsteins.dm ⁻³ .min ⁻¹)	(a) 1.284	4.004	2	0.092	0.26
			4	0.117	
			8	0.143	
			10	0.150	
			12	0.165	
			14	0.219	
365 nm , laser ($I_0 = 3.6209 \times 10^3$ einsteins.dm ⁻³ sec ⁻¹)	(b) 1.435	3.630	1	0.055	0.37
			2	0.081	
			3	0.100	
			4	0.135	
			5	0.149	
	(c) 1.435	1.815	1	0.020	0.35
			2	0.050	
			3	0.075	
			4	0.100	
			5	0.125	
370 nm , laser ($I_0 = 3.6209 \times 10^3$ einsteins.dm ⁻³ sec ⁻¹)	(d) 1.435	3.630	1	0.080	0.34
			2	0.105	
			3	0.125	
			4	0.150	
			5	0.160	
			6	0.200	
	(e) 1.435	1.815	1	0.035	0.29
			2	0.055	
			3	0.070	
			4	0.095	
			5	0.090	
			6	0.120	

It can be concluded that the thermal path of the reaction involves an AB type adduct whose formation constants, obtained from kinetic data at four different temperatures, yield an enthalpy of formation equal in magnitude to those of typical EDA complexes. This supports the assumption of an EDA intermediate in the reaction. The photochemical reaction, however, proceeds with radiation of wavelengths 360, 365 and 370 nm which are within the $n-\pi^*$ absorption band of 2,3-dichloro 1,4-naphthoquinone (A). At these wavelengths DPTU has no absorption. Hence the photochemical process is initiated by the excited A. Use of laser beam increases the rate but does not change the quantum yield, meaning thereby that the mechanism under laser irradiation is the same as that under ordinary light.